J. Anat. (2006) **208**, pp353–359

Error estimation of the fractal dimension measurements of cranial sutures

Andrzej Z. Górski[1] and Janusz Skrzat[2]

[1]*Institute of Nuclear Physics, Polish Academy of Sciences, Krakow, Poland*
[2]*Department of Anatomy, Collegium Medicum, Jagiellonian University, Krakow, Poland*

Abstract

The fractal exponents used to quantify the complexity of cranial sutures were computed for 17 coronal and 17 sagittal sutures of adults from different populations, using the box-counting algorithm. This paper discusses the main sources of error for the fractal exponents, and gives the error estimates. We then compare our results with those obtained by other authors. We suggest that the usual error estimates implied by the standard deviation for the regression line are too low. We emphasize the crucial role played by the choice of regression line in the log–log plot. For the coronal and sagittal sutures we found mean fractal dimensions of 1.48 and 1.56, respectively. Our values are close to the value for Brownian random walk.

Key words cranial sutures; fractal measures; frontal bone; parietal bone; sutural complexity.

Introduction

The coronal and sagittal sutures facilitate proper cranial growth and expansion of the cerebral hemispheres. It is well known that these sutures are a type of fibrous joint in which the apposed bony surfaces are so closely united by a thin layer of fibrous connective tissue that only limited movement can occur. The coronal suture extends across the skull between the two parietal bones and the frontal bone. This enables elongation of the cranial vault. The sagittal suture joins the right and left parietal bones and facilitates transverse cranial growth (Oudhof, 1982; Persson, 1995). The coronal and sagittal sutures serve as the major growth centres and articulate bones of the neurocranium (Opperman, 2000). The sutural morphology is strongly related to the extra- and intracranial forces generated during head growth (Moss, 1957).

Morphologically, these bony formations resemble irregular curves, which may vary locally from nearly straight lines to extremely convoluted sinusoids or even loops. Visually, cranial sutures resemble fractal structures. In principle, any geometric object can be non-fractal, monofractal or multifractal (Mandelbrot, 1983). Fractal objects have the following property: parts of the set – properly rescaled (magnified), and possibly with different scaling factors in different directions (for self-affine fractals) – are identical. They are perfectly identical in the case of deterministic fractals. In the real world we are more likely to encounter statistical fractals, where the rescaled parts have the same statistical properties as the whole object. In particular, cranial sutures are statistical fractals. For statistical fractals, determination of fractal dimensions is usually less accurate than for deterministic fractals. Both deterministic and statistical fractals can be either monofractals or multifractals. Multifractal sets are more complicated; they can be viewed as a superposition of many fractal sets with different fractal dimensions, and they are characterized by infinite multiplicity of generalized fractal exponents. There is a very large diversity of monofractals and it is possible to construct two monofractal curves that differ far more than a multifractal curve differs from a monofractal curve. Hence, it is not possible to distinguish between the two cases by visual inspection, and computational methods should be applied.

There have been several attempts to calculate the fractal dimensions of cranial sutures (Tsonis & Tsonis,

Correspondence
Dr Janusz Skrzat, Department of Anatomy, Collegium Medicum, Jagiellonian University, Kopernika 12, 31-034 Krakow, Poland.
E: jskrzat@poczta.onet.pl

Accepted for publication *2 November 2005*

1987; Long & Long, 1992; Lynnerup & Jacobsen, 2003; Skrzat & Walocha, 2003; Yu et al. 2003). However, there are quite considerable discrepancies in the results obtained by different authors, with the suggested fractal dimension ranging from physically impossible values below 1.0 up to the values above 1.6 (Lynnerup & Jacobsen, 2003).

We suspect that one important factor in these differences is the use of 'black box' commercial software to estimate fractal dimension. Therefore, the aim of this study was to perform a careful analysis of the fractality of cranial sutures using our own box-counting code, paying more attention to fitting the regression line in the log–log plot. We set out to determine whether the cranial sutures are monofractal, multifractal or non-fractal structures; we estimated the expected accuracy of these calculations; and finally we estimated the fractal dimensions of the coronal and sagittal sutures.

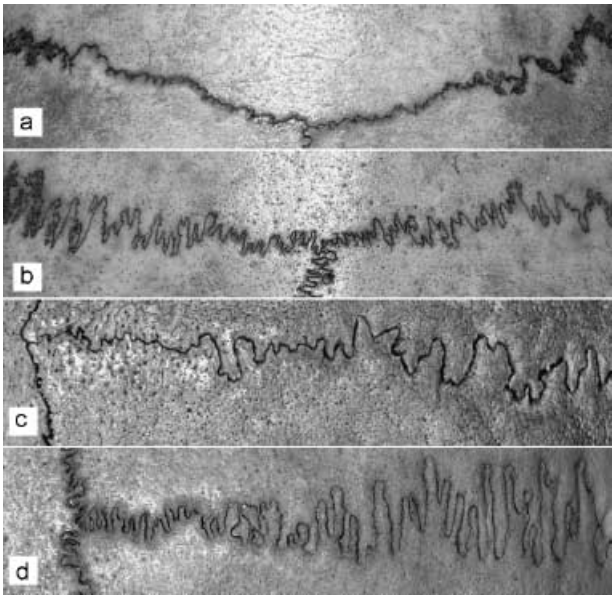

Fig. 1 The least and the most complicated coronal (a,b) and sagittal sutures (c,d) of the analysed cranial set.

Materials and methods

We analysed the coronal and sagittal sutures of 17 adult skulls (13 males, four females) from different populations. The cranial set that we investigated presents considerable morphological variation caused by diversified ethnicity. The skulls are stored at the Department of Anatomy of Collegium Medicum of Jagiellonian University, Krakow, Poland.

All the sutures we examined, and their contours, were clearly visible and undamaged (Fig. 1). The portion of the coronal and sagittal suture that was visible at the superior aspect of the cranial vault was photographed using a digital camera. The fractal dimension was computed for one pixel line that was extracted from the suture contours with the aid of graphics software. The pixels were digitalized to two-dimensional (2D) coordinates. We used our own dedicated box-counting code instead of commercial software to enable us to control the subtleties of the intermediate steps. The generalized fractal dimensions were computed applying the standard box-counting algorithm to the digitized data. This gives the corresponding points in the standard log–log plot. However, the points used for the linear regression were chosen manually. For each suture we computed several neighbouring fits, choosing the best one, in order to minimize the χ^2 parameter (a sum of the squared deviations from the fit) and to minimize the influence of the boundary conditions.

A fractal dimension of a curve is a non-integer number, which in principle may vary between 1.0 (a smooth curve) and 2.0 (extremely erratic data, e.g. white noise). The Brownian random walk (BRW) has an intermediate value fractal dimension equal to 1.5. Greater fractal dimension values are usually related to higher complexity of the underlying structures. Considering a cranial suture as a fractal makes it possible to classify its morphological structure and level of complexity based on the value of its fractal dimension. We have assumed that sutures are 2D objects, as the skull's surface is relatively smooth and the fractal dimension is invariant with respect to smooth transformations. Hence, the numerical data can be viewed as a local projection of sutures to the tangent x–y-plane, and our initial numerical data are sets of the coordinates (x, y). The number of data points (n_{tot}) in each set varies within the interval 9 000–29 000, with the average of above 16 000. For 2D sets, this is not a very large number and determination of the best fit for the log–log plot should be performed very carefully.

The box-counting algorithm and its pitfalls

To determine the fractal properties of our data we used the standard box-counting algorithm for sets embedded in 2D planes. The box-counting algorithm successively divides the data set into smaller and smaller squares

(the linear ratio is usually taken to be 1/2). This procedure is repeated N times. The number N should not be too large, because for sufficiently small 'boxes' (squares) there is only one data point in each box and the subsequent divisions give the same contribution to the algorithm, leading to the fractal dimension approaching zero (see the sum in Eq. 1 below). Hence, if N is too large, it can give us unrealistically small numbers. It is clear that this was the case for Lynnerup & Jacobsen (2003), where the authors reported physically impossible low fractal dimensions below 1.0. This result is theoretically impossible for any curve. This effect can be more subtle, leading to results that are apparently more realistic but still too low. In addition, the largest box (division $N = 1$), containing the whole set, also gives the incorrect contribution to the fractal dimension. In the log–log plot this will always be the point with coordinates (0,0), whatever data we take into account. To summarize, for a good estimate of the fractal dimension one must take into account divisions at least of the order of $N_{\min} > 1$, and at most of the order of $N_{\max}$. $N_{\max}$ can be estimated by checking the average number of data points per one non-empty box. This number must be considerably greater than one (Molteno, 1993; Górski, 2001). In addition, to call the set a 'fractal', a good scaling should be apparent within the range from $N_{\min}$ to $N_{\max}$, i.e. an excellent linear fit in the log–log plot.

To find a multifractal structure instead of a single fractal dimension (d), an infinite set of fractal exponents $d(q)$ is used (they are also called the generalized fractal dimensions). Mathematically they are defined by the following formula (Hentschel & Procaccia, 1983; Górski, 2001):

$$d(q) = \frac{1}{1-q} \lim_{N\to\infty} \frac{\ln \sum_i p_i^q(N)}{\ln(2^N)}. \qquad (1)$$

Here, N enumerates successive divisions of a plane into squares ('boxes'), $i = i(N)$ counts the boxes for a given division and $p_i(N)$ denotes the fraction of the data points contained in the ith box (of a given division, N). The numbers $p_i(N)$ can be interpreted as probabilities of finding a data point in the ith box of the division N. In principle, the parameter q can be any number from minus to plus infinity. However, the most common choices for q are 0, 1 and 2. They are called capacity, information and correlation dimension, respectively. By changing the parameter q one 'scans' the structure of the multifractal. A large q gives more weight to large probabilities $p_i(N)$, whereas a small q enhances small probabilities $p_i(N)$. Therefore, for larger q-values the dimension $d(q)$ is more sensitive to noise, increasing errors.

The quantities $d(q)$ are extracted from the log–log plot of N vs. $\ln Y_q(N)$, where the latter quantity (see Eq. 1) is defined as:

$$\ln Y_q(N) = \frac{1}{1-q} \ln \sum_i p_i^q(N). \qquad (2)$$

We compute $d(q)$ from the slope of the regression line. The exponents $d(q)$ do exist if for a reasonable range of successive divisions one can find a good linear fit in the log–log plot (see Fig. 2). This implies good scaling properties and the fractal nature of our object.

For monofractal sets all the above exponents are identical: $d(q) = d = const.$ If one can find a good scaling and different values for $d(q)$, this set is termed multifractal. For non-fractal objects a good linear fit cannot be found at all, and the mathematical limit in the formula for $d(q)$ does not exist. Clearly, for practical calculations we can use the above formula only for $N < N_{\max}$, the infinite limit cannot be reached and the fractal behaviour cannot be proven in the mathematical sense. Usually in practical calculations several points

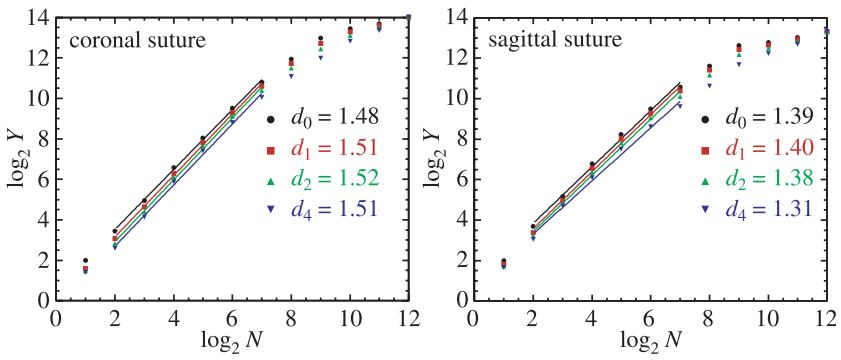

Fig. 2 The log–log plots used to extract fractal dimensions of the coronal and sagittal sutures in the case of the six-point fit. Fits for d_q with $q = 0$, 1, 2 and 4 are displayed in the graphs. The vertical axis represents the expression defined by Eq. (2). The horizontal axis enumerates the successive divisions.

are taken into account, at best up to 8–10 points. The upper limit is related to the number of data points (n_{tot}). In addition, for multifractals there is a mathematical theorem that $d(q)$ must be a monotonically decreasing or a constant function. This is one of the possible ways to check whether we are dealing with a real fractal, or if the scaling is merely an artefact (Górski, 2001).

In our computations we have processed the data for 34 sutures, calculating the generalized dimensions $d(q)$ for values of q = 0, 1, 2 and 4. Higher values of q are more sensitive to the noise generated by technical limitations. The value q = 4 has been used in an extra test of the accuracy of our calculations. In addition, we have found that the sample data do not meet the condition of normal distribution and their variations are unequal. Thus, a non-parametric Mann–Whitney test was applied to verify null hypotheses, which states that complexities expressed by fractal dimensions of the coronal and sagittal suture are equal. The statistical analysis was performed using Statistica software (StatSoft, 2003).

Numerical results

Our calculations of the fractal dimensions of the coronal and sagittal sutures show clearly that average differences $|d(0) - d(1)|$ and $|d(1) - d(2)|$ for the coronal and sagittal sutures are equal to about 0.01, which is negligible in comparison with the estimated accuracy. Hence, we have accepted that $d(q)$ is constant. This suggests a good monofractal scaling within the investigated range (two orders of magnitude, Fig. 2). The difference $|d(2) - d(4)|$ calculated for all fits in the case of coronal and sagittal sutures equals 0.02 and 0.07, respectively. Thus, the coronal sutures seem to be less 'noisy'. This effect is due partly to the data series, which are about 15% longer for the sagittal sutures. It may also result from better scaling of the coronal data series. Because the calculations are increasingly more sensitive to noise as q increases, this supports the view that we have found good monofractal scaling.

To compute fractal exponents and its accuracy we have performed several linear fits for each of the 34 sutures, taking into account different sets of points in the log–log plot (see Fig. 2 as an example of the six-point fit). The five-point fit to the log–log plot gives a systematic difference in comparison with the six-point fit, on average about +0.02 for the coronal and +0.08 for the sagittal sutures. This indicates that we are approaching the boundary of scaling for the six-point fit. We also have better scaling for the coronal sutures, where the number of data points was higher. The other choices of fitted points were definitely worse. Taking into account points with N = 8 we approach the saturation region, and the values obtained from the regression are considerably lower (due to the finite nature of the sample, for large N and for any data, one obtains a horizontal line and the regression implies values approaching zero). This effect can be seen in Fig. 2, where points with larger N tend to have a lower slope.

Our results support the proposition that coronal and sagittal sutures have fractal properties, which should be regarded as stochastic monofractal sets. Hence, the linear scaling is visible in the range $1 : 2^6$, i.e. for almost three orders of magnitude. Similar conclusions can be obtained independently by qualitative analysis of the raw input data. The size of the whole suture is (in magnitude) about 100 mm. By contrast, its finest details that can be taken into account are definitely greater than 0.1 mm. Hence, any reasonable scaling range must be smaller than three orders of magnitude. This implies the regression fit for about 5–6 points in the log–log plot.

From this analysis the accuracy of our calculations for $d(q)$ can be safely estimated as being about ± 0.05 or better (i.e. about 3–4%). This was deduced from the comparison of neighbouring regression lines. This is in strong contrast to the standard deviation calculated for the fits. The χ^2 parameter (a sum of the squared deviations from the fit) implies that the fractal dimension accuracy is about ± 0.01 and ± 0.02 for the fractal dimension accuracy, for the coronal and sagittal sutures, respectively. This shows that comparison of neighbouring regression lines is a more reliable way of estimating the accuracy of the box-counting algorithm. In addition, as was stressed in the previous section, we have found that shifting the choice of fitted points in the log–log plot (Fig. 2) by one or two points can considerably change the final result. In our view, this is the most delicate part of the procedure.

Similar conclusions concerning accuracy can be qualitatively obtained by analysing the length of the input data series. For the Gaussian data the standard error can usually be estimated as being of the order of $1/\sqrt{(n_{tot})}$, where n_{tot} is the total number of data points. For cranial sutures this number is usually of the order of 10^4, leading to an error estimate of the order of 1%. However, in this case, instead of a simple Gaussian distribution

we have a complicated 2D geometrical structure. Hence, we can expect a much larger error estimate, in qualitative accordance with our results. The problem of error estimates for fractal dimensions is very complicated, and beyond the scope of this paper (Molteno, 1993; Górski, 2001).

The averages of our results for the fractal dimensions of coronal and sagittal sutures are compared in Table 1 and Fig. 3. The range of coronal suture complexity overlaps with that of sagittal suture complexity. Sagittal sutures have higher mean fractal dimension than coronal sutures.

The computed result of the Mann–Whitney test allowed us to reject the null hypothesis, which assumes that the complexity of the coronal and sagittal sutures is equal. Taking into account statistically significant differences between sum ranks of fractal dimensions (Table 2) and visual inspection of the sutures, we conclude that the analysed sutures are morphologically distinct.

Table 1 Comparison of sutural complexity of the coronal and sagittal sutures expressed by fractal dimension

Suture	Mean	Min.	Max.	SD
Sagittal	1.56	1.43	1.63	0.060
Corona	1.48	1.30	1.64	0.105

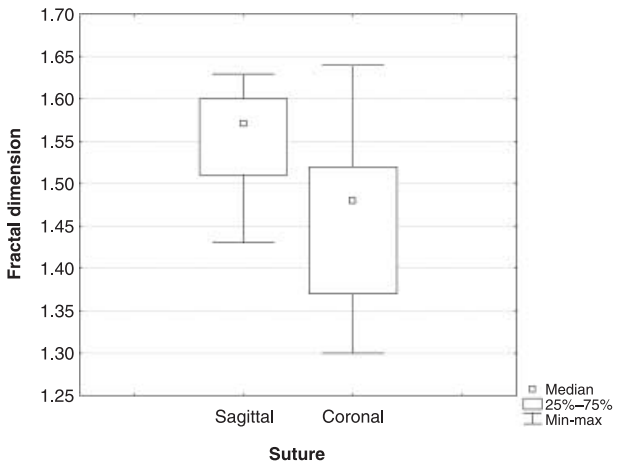

Fig. 3 Box-and-whisker plot of the variation of the fractal dimension between coronal and sagittal sutures.

Discussion and conclusions

The fractal structure of a cranial suture is mainly due to the spatial organization of minute bony projections, which arise from the edges of the frontal and parietal bones. Opposing edges of the frontal and parietal bones meet within the suture, forming interdigitation of various levels of complexity. Because the patterns of the right and left coronal sutures (from bregma to stephanion) are similar, we treated these parts together. Thus, we obtained twice as many data points for the fractal dimension estimates, and this increased its accuracy. The average number of data points was 17 963 for coronal sutures and 15 667 for sagittal sutures.

Visual inspection of the coronal and sagittal sutures reveals a non-uniform character of the suture interdigitation and various distributions of the bony projections along the course of the suture. There are segments of the suture that only slightly resemble a sinusoid line, whereas the rest of the suture can be extremely convoluted. This makes it difficult to score overall complexity visually, and also to compare such irregular patterns of different skulls. The fractal dimension is a good quantitative measure of sutural morphology.

We decided to test error estimates for computation of fractal dimensions using coronal and sagittal sutures because they are relatively long and distinct, and they have fractal structure, which means that they yield an adequate data set for numerical analysis. Because fractal analysis of cranial sutures has already been undertaken by other authors, we were able to compare our results and analyse the discrepancies that appear in calculations of fractal dimensions when the box-counting algorithm is applied. According to Long & Long (1992), intricate sagittal sutures show 2–3 orders of self-similarity in a wavy line and yield fractal dimensions of about 1.3–1.4. Our results, and our previous study on the

Table 2 Result of Mann–Whitney test for the fractal dimension of coronal and sagittal sutures

Rank sum coronal	Rank sum sagittal	*U*	*Z*	*P*	*Z* adjusted	*P*	Valid *N* coronal	Valid *N* sagittal
358 500	236 500	83 500	2101*	0.036*	2105*	0.035*	17	17

*Statistically significant.

complexity of sagittal sutures, confirm this observation (Hartwig, 1991; Lynnerup & Jacobsen, 2003; Skrzat & Walocha, 2003; Yu et al. 2003). Lynnerup & Jacobsen (2003) found that mean fractal dimensions were relatively low for coronal sutures (1.106 for female skulls, 1.118 for male skulls) and sagittal sutures (1.049 for female skulls, 1.161 for male skulls). Our mean fractal dimensions for these two types of sutures are significantly higher (1.48 and 1.56 for coronal and sagittal sutures, respectively, estimated for both sexes together). In our view, these large differences may result from differences in the choice of points for the regression line in the box-counting algorithm. Physically impossible results ($d < 1.0$) reported by Lynnerup & Jacobsen (2003) strongly support this hypothesis.

Detailed analysis shows that the cranial sutures are geometrically monofractal objects with their fractal dimension oscillating around 1.5. The key factor in fractal analysis based on the box-counting algorithm is the proper choice of points in the log–log plot for the regression line. To calculate reliable fractal exponents we repeated our calculations for each suture at least three times, fitting the straight line for five, six and seven points, respectively. In our opinion, the six-point fit, as shown in Fig. 2, was the most reliable. The difference between those fits (about 3–4%) provides a good accuracy estimate of our results. This is in contrast to the relatively small standard deviation obtained for each single fit. In our view this is the main cause of the relatively large differences in the results obtained by different authors. Our error estimate is quite close to the standard deviation for fractal dimensions of the whole set of different sutures.

The accuracy of the finest details of cranial sutures can be measured within the range 0.1–0.5 mm. The size of the whole sample is of the order of 100 mm. This gives, at most, three orders of magnitude of theoretically possible scaling. Hence, the resulting maximum number of fitted points in the log–log plot should be well below 10 ($2^{10} = 1024 \sim 10^3$). This implies that the expected acceptable scaling cannot extend much above the range of about two orders of magnitude, as in our study. In our case, the number of points in the log–log plot that is within the reasonable linear scaling range equals 5–7 (Fig. 2). As can be seen from the plot, the saturation of scaling is clearly visible for $N = 10$. Taking into account the points from $N = 3$ up to $N = 9$, we have found that the results deviate considerably from the case when the scaling exponents are calculated up to the $N = 8$ and $N = 7$ subdivisions. This is consistent with the fact that, in the subdivision with the factor $2^9 = 512$, the details below 0.5 mm became important. The best linear fit is reached with six points. The χ^2 parameter for d_0 was below 0.05 in most cases. Typically, it was much better for the coronal sutures (on average 0.004 and 0.005 for six- and five-point fits, respectively, leading to the expected 'theoretical' accuracy of d_q below 0.01). For the sagittal sutures the corresponding values are 0.05 and 0.02, which implies uncertainty for d_0 below 0.02.

By contrast, results for the mean fractal dimensions of sagittal sutures estimated by Yu et al. (2003) were 1.29, and at the 95% confidence level they were between 1.28 and 1.31. Their analysis was based on the standard deviations for a given linear regression, and the differences with the 'neighbouring fits' were not calculated. These values may be due to the smoothness of the sutures in their sample. In our view, however, these results may also be so low because of problems with the choice of fitted points.

In conclusion, we suggest that more careful and extensive investigation of fractal exponents of sutures is necessary, and that special attention should be paid to the linear fits in the log–log plots. The error estimates should also be done more carefully, taking into account the neighbouring fits instead of the standard deviation for a given regression line. In this context, investigation of differences between different sexes, ethnic groups, etc., seems to be premature. This also applies to investigations of different parts of a single suture. Here, the number of data points is much smaller and the results are less reliable. The good news is that according to our analysis the cranial sutures seem to be monofractal, and that the computations are more reliable than for multifractals, where contributions from different data subsets must be extracted. The precise determination of fractal dimensions may also be important for future models of suture formation.

References

Górski AZ (2001) Pseudofractals and box counting algorithm. *J Phys (GB)* **A34**, 7933–7941.

Hartwig WC (1991) Fractal analysis of sagittal suture morphology. *J Morph* **210**, 289–290.

Hentschel HE, Procaccia I (1983) The infinite number of generalised dimensions of fractals and strange attractors. *Physica* **D8**, 435–444.

Long CA, Long JE (1992) Fractal dimensions of cranial sutures and waveforms. *Acta Anat* **145**, 201–206.

Lynnerup N, Jacobsen JC (2003) Age and fractal dimension of sagittal and coronal suture. *Am J Phys Anthropol* **121**, 332–336.

Mandelbrot BB (1983) *The Fractal Geometry of Nature*. New York: Freeman.

Molteno TCA (1993) Fast O(N) box counting algorithm for estimating dimensions. *Phys Rev* **E48**, R3263–R3266.

Moss ML (1957) Experimental alteration of sutural area morphology. *Anat Rec* **127**, 569–589.

Opperman LA (2000) Cranial sutures as intramembranous bone growth sites. *Dev Dyn* **219**, 472–485.

Oudhof HA (1982) Sutural growth. *Acta Anat* **112**, 58–68.

Persson M (1995) The role of sutures in normal and abnormal craniofacial growth. *Acta Odontol Scand* **53**, 152–161.

Skrzat J, Walocha J (2003) Fractal dimensions of the sagittal (interparietal) sutures in humans. *Folia Morph (Warsz)* **62**, 119–122.

StatSoft Inc. (2003) *STATISTICA (Data Analysis Software System)*, Version 6. www.statsoft.com.

Tsonis AA, Tsonis PA (1987) Fractals: a new look at biological shape and patterning. *Persp Biol* **30**, 355–361.

Yu JC, Wright RL, Williamson MA, Braselton JP, Abell M (2003) A fractal analysis of human cranial sutures. *Cleft Palate Craniofac J* **40**, 409–415.